Evidence for the Appearance of Atmospheric Tau Neutrinos in Super-Kamiokande

K. Abe *et al.* (Super-Kamiokande Collaboration)

Phys. Rev. Lett. **110**, 181802 — Published 2 May 2013

DOI: 10.1103/PhysRevLett.110.181802

Evidence for the Appearance of Atmospheric Tau Neutrinos in Super-Kamiokande

K. Abe,[1,27] Y. Hayato,[1,27] T. Iida,[1] K. Iyogi,[1] J. Kameda,[1,27] Y. Koshio,[1,27] Y. Kozuma,[1] Ll. Marti,[1] M. Miura,[1,27] S. Moriyama,[1,27] M. Nakahata,[1,27] S. Nakayama,[1,27] Y. Obayashi,[1,27] H. Sekiya,[1,27] M. Shiozawa,[1,27] Y. Suzuki,[1,27] A. Takeda,[1,27] Y. Takenaga,[1] K. Ueno,[1] K. Ueshima,[1] S. Yamada,[1] T. Yokozawa,[1] C. Ishihara,[2] H. Kaji,[2] T. Kajita,[2,27] K. Kaneyuki,[2,27,*] K.P. Lee,[2] T. McLachlan,[2] K. Okumura,[2] Y. Shimizu,[2] N. Tanimoto,[2] L. Labarga,[3] E. Kearns,[4,27] M. Litos,[4] J.L. Raaf,[4] J.L. Stone,[4,27] L.R. Sulak,[4] M. Goldhaber,[5,*] K. Bays,[6] W.R. Kropp,[6] S. Mine,[6] C. Regis,[6] A. Renshaw,[6] M.B. Smy,[6,27] H.W. Sobel,[6,27] K.S. Ganezer,[7] J. Hill,[7] W.E. Keig,[7] J.S. Jang,[8,†] J.Y. Kim,[8] I.T. Lim,[8] J.B. Albert,[9] K. Scholberg,[9,27] C.W. Walter,[9,27] R. Wendell,[9] T.M. Wongjirad,[9] T. Ishizuka,[10] S. Tasaka,[11] J.G. Learned,[12] S. Matsuno,[12] S.N. Smith,[12] T. Hasegawa,[13] T. Ishida,[13] T. Ishii,[13] T. Kobayashi,[13] T. Nakadaira,[13] K. Nakamura,[13,27] K. Nishikawa,[13] Y. Oyama,[13] K. Sakashita,[13] T. Sekiguchi,[13] T. Tsukamoto,[13] A.T. Suzuki,[14] Y. Takeuchi,[14,27] M. Ikeda,[15] A. Minamino,[15] T. Nakaya,[15,27] Y. Fukuda,[16] Y. Itow,[17,18] G. Mitsuka,[17] T. Tanaka,[17] C.K. Jung,[19] G.D. Lopez,[19] I. Taylor,[19] C. Yanagisawa,[19] H. Ishino,[20] A. Kibayashi,[20] S. Mino,[20] T. Mori,[20] M. Sakuda,[20] H. Toyota,[20] Y. Kuno,[21] M. Yoshida,[21] S.B. Kim,[22] B.S. Yang,[22] H. Okazawa,[23] Y. Choi,[24] K. Nishijima,[25] M. Koshiba,[26] M. Yokoyama,[26,27] Y. Totsuka,[26,*] K. Martens,[27] J. Schuemann,[27] M.R. Vagins,[27,6] S. Chen,[28] Y. Heng,[28] Z. Yang,[28] H. Zhang,[28] D. Kielczewska,[29] P. Mijakowski,[30] K. Connolly,[31] M. Dziomba,[31] E. Thrane,[31,‡] and R.J. Wilkes[31]

(The Super-Kamiokande Collaboration)

[1]*Kamioka Observatory, Institute for Cosmic Ray Research, University of Tokyo, Kamioka, Gifu 506-1205, Japan*
[2]*Research Center for Cosmic Neutrinos, Institute for Cosmic Ray Research, University of Tokyo, Kashiwa, Chiba 277-8582, Japan*
[3]*Department of Theoretical Physics, University Autonoma Madrid, 28049 Madrid, Spain*
[4]*Department of Physics, Boston University, Boston, MA 02215, USA*
[5]*Physics Department, Brookhaven National Laboratory, Upton, NY 11973, USA*
[6]*Department of Physics and Astronomy, University of California, Irvine, Irvine, CA 92697-4575, USA*
[7]*Department of Physics, California State University, Dominguez Hills, Carson, CA 90747, USA*
[8]*Department of Physics, Chonnam National University, Kwangju 500-757, Korea*
[9]*Department of Physics, Duke University, Durham NC 27708, USA*
[10]*Junior College, Fukuoka Institute of Technology, Fukuoka, 811-0214, Japan*
[11]*Information and Multimedia Center, Gifu University, Gifu, Gifu 501-1193, Japan*
[12]*Department of Physics and Astronomy, University of Hawaii, Honolulu, HI 96822, USA*
[13]*High Energy Accelerator Research Organization (KEK), Tsukuba, Ibaraki 305-0801, Japan*
[14]*Department of Physics, Kobe University, Kobe, Hyogo 657-8501, Japan*
[15]*Department of Physics, Kyoto University, Kyoto, Kyoto 606-8502, Japan*
[16]*Department of Physics, Miyagi University of Education, Sendai, Miyagi 980-0845, Japan*
[17]*Solar Terrestrial Environment Laboratory, Nagoya University, Nagoya, Aichi 464-8602, Japan*
[18]*Kobayashi-Maskawa Institute for the Origin of Particle and the Universe, Nagoya University, Nagoya, Aichi 464-8602, Japan*
[19]*Department of Physics and Astronomy, State University of New York, Stony Brook, NY 11794-3800, USA*
[20]*Department of Physics, Okayama University, Okayama, Okayama 700-8530, Japan*
[21]*Department of Physics, Osaka University, Toyonaka, Osaka 560-0043, Japan*
[22]*Department of Physics, Seoul National University, Seoul 151-742, Korea*
[23]*Department of Informatics in Social Welfare, Shizuoka University of Welfare, Yaizu, Shizuoka, 425-8611, Japan*
[24]*Department of Physics, Sungkyunkwan University, Suwon 440-746, Korea*
[25]*Department of Physics, Tokai University, Hiratsuka, Kanagawa 259-1292, Japan*
[26]*The University of Tokyo, Bunkyo, Tokyo 113-0033, Japan*
[27]*Kavli Institute for the Physics and Mathematics of the Universe (WPI), University of Tokyo, Kashiwa, Chiba, 277-8583, Japan*
[28]*Department of Engineering Physics, Tsinghua University, Beijing, 100084, China*
[29]*Institute of Experimental Physics, Warsaw University, 00-681 Warsaw, Poland*
[30]*National Centre For Nuclear Research, 00-681 Warsaw, Poland*
[31]*Department of Physics, University of Washington, Seattle, WA 98195-1560, USA*

Super-Kamiokande atmospheric neutrino data were fit with an un-binned maximum likelihood method to search for the appearance of tau leptons resulting from the interactions of oscillation-generated tau neutrinos in the detector. Relative to the expectation of unity, the tau normalization is found to be $1.42 \pm 0.35\ (stat)\ ^{+0.14}_{-0.12}\ (sys)$ excluding the no-tau-appearance hypothesis, for which the normalization would be zero, at the 3.8σ level. We estimate that $180.1 \pm 44.3\ (stat)\ ^{+17.8}_{-15.2}\ (sys)$ tau leptons were produced in the 22.5 kton fiducial volume of the detector by tau neutrinos during the 2806 day running period. In future analyses, this large sample of selected tau events will allow the study of charged current tau neutrino interaction physics with oscillation produced tau neutrinos.

PACS numbers: 14.60.Pq, 96.40.Tv
Keywords: Neutrino Oscillations, Super-Kamiokande, Tau Neutrinos, Atmospheric Neutrinos

It is now well known that neutrinos undergo flavor oscillations. The flavor states of the neutrino measured through the weak interaction are quantum mechanical mixtures of neutrino mass states. As observed in the quark sector, this mixture results in oscillations of detected flavor states. Evidence exists for this effect in atmospheric neutrinos [1, 2], solar neutrinos [3–7], reactor experiments [8], and long-baseline oscillation experiments [9–11]. In 2011, the T2K [12], MINOS [13], and Double Chooz [14] experiments showed the first indications of full three-flavor oscillations. In 2012 the Daya Bay [15] and RENO [16] experiments reported the first precision measurements of the θ_{13} mixing angle which drives three-flavor oscillation.

Definitive proof of flavor oscillation requires unambiguous appearance of the charged current interaction of a neutrino not in the original source. In the dominant oscillation for ν_μ at GeV energies, $\nu_\mu \to \nu_\tau$ oscillations, observing the resulting τ lepton is quite difficult. This is because producing a tau lepton requires a neutrino of energy greater than a threshold of 3.5 GeV. Long-baseline experiments tuned to the neutrino oscillation maximum for their distances tend to have the bulk of their neutrinos below this energy. Furthermore, the tau lepton immediately decays to final states with an electron, muon or mesons plus a tau neutrino so the tau lepton itself cannot be easily seen. Nevertheless, the OPERA collaboration was recently able to show evidence for a single reconstructed event in their emulsion consistent with tau appearance [17]. The Super-K collaboration first published a search for tau appearance in atmospheric neutrinos in 2006 [18]. Since the atmospheric neutrino flux extends to energies well above 10 GeV, and spans a wide range of baselines, we expect to see tau leptons produced in the Super-K detector. However, these events must be distinguished from other high-energy atmospheric neutrino interactions. Further comparisons of these techniques can be found in [19] and prospects for future detectors can be found in [20].

This letter reports a result from a new search utilizing the Super-Kamiokande experiment. This analysis addresses the question of whether the atmospheric data is consistent with lack of oscillation-generated ν_τ, or whether they are necessary to explain the observations. Super-Kamiokande (Super-K) is a 50,000 ton water Cherenkov detector[21] with 22.5 ktons of fiducial volume. It consists of two concentric detectors: a inner-detector with 11,129 inward-looking 20 inch photo-detectors, and an outer-detector with 1885 outward-facing 8 inch photo-detectors which acts as a veto. Its large target mass makes it well suited to look for the rare appearance of tau neutrinos from oscillations. The typical energy of atmospheric neutrinos is about 1 GeV. Due to the previously noted energy threshold, about one ν_τ charged current event per kton-year should be produced in the Super-K detector.

Super-K has been in operation for approximately fifteen years and has had several running configurations indicated by the labeling SK-I (1996-2001), SK-II (2002-2005), SK-III (2006-2008) and SK-IV (2008-2012). The previously reported Super-K result [18] was based on the data from SK-I alone. Since that time the analysis has been improved to increase its sensitivity and the data set used has been expanded to also include SK-II and SK-III, thereby almost doubling its size. As the total data set covers the period between 1996 and 2008, it comprises 2806 days of live-time.

In order to predict the rate of both the tau signal and atmospheric background, a full Monte Carlo (MC) simulation is used both to predict the neutrino interactions inside the detector and to model the response of Super-K itself. Three-dimensional neutrino fluxes for ν_μ and ν_e produced in atmospheric showers are taken from the flux calculation of Honda *et al.* [22]. The fluxes are oscillated with a custom code [23] which takes into account all relevant path lengths, energies and matter effects using our current knowledge of three-flavor neutrino oscillation parameters. The oscillation parameters used are [24–26]: $\Delta m^2_{32} = 2.1\times10^{-3}\mathrm{eV}^2$, $\Delta m^2_{21} = 7.6\times10^{-5}\mathrm{eV}^2$, $\sin^2 2\theta_{23} = 1.0$, $\sin^2 2\theta_{12} = 0.84$, $\delta_{\mathrm{CP}} = 0$. The Super-K best fit value of Δm^2_{32} from [24, 25] was used in order to make use of the full set of systematic errors which were previously evaluated around this point. However, the difference in results between using this value and that of recent more precise values reported in the literature [27] is found to be negligible due to the wide range of L and E sampled by the atmospheric neutrinos. For the values of θ_{13}, recent Daya Bay [15] and RENO [16] results are combined in a weighted average and we use $\sin^2 2\theta_{13} = 0.099$. The interactions of the ν_μ, ν_e, and oscillation-produced ν_τs with the nuclei of water molecules inside of the Super-K detector are modeled with the NEUT [2, 28] neutrino interaction code. Finally, a GEANT3 [29] based detector MC is used to simulate Super-K itself. More detailed descriptions of this software can be found in [2].

For the purposes of this analysis it is important to understand some details of the neutrino interaction model. The NEUT code models the known neutrino-nucleon interactions including quasi-elastic scattering, single meson production, coherent pion production, and deep-inelastic scattering (DIS). All ν_μ and ν_e interactions are simulated. Additionally, charged-current (CC) ν_τ interactions are simulated and added to the sample using weighting based on the oscillation probabilities. Neutral current (NC) interactions are assumed to be unaffected by oscillations. The ν_τ CC cross-sections are calculated following the same models as those used for ν_μ and ν_e with the appropriate lepton mass terms. In the case of single and coherent pion production lepton mass corrections not included in the original models are also employed [30, 31]. Tau leptons are decayed using TAUOLA (Version 2.6) [32]. Since the distribution of decay particles depends on the polarization of the tau lepton, a polarization model from [33] is incorporated into NEUT. At the relevant neutrino energies selected by this analysis, the CC interactions contain a high percentage of DIS (46%) with the portion of CC events induced by the ν_τ signal interactions alone containing 56% DIS. In the calculation of the cross sections of DIS, the GRV94 [34] parton distribution functions are used, and additional corrections to make the DIS cross-sections match smoothly with the resonance region as developed by Bodek and Yang are also applied [35]. More details of the DIS implementation can be found in [2].

The signature of oscillation-induced tau neutrinos in the atmospheric flux is the detection of the decay of tau leptons in the Super-K detector. As the leptonic decays of the tau look on the whole very similar to normal CC DIS interactions from ν_μ and ν_e, an analysis is developed which attempts to select the hadronic decays.

In order to select the tau events, we first identify high energy events contained in the inner detector by requiring that there is no appreciable activity in the outer detector, the interaction is in the fiducial volume (the distance to the nearest wall > 200 cm), and the event has more than 1.3 GeV of visible energy. The selection efficiencies for this set of cuts are 81% for the ν_τ CC signal and 23% for the background events respectively.

The presence of the extra pions from hadronic tau decay which come from a heavy object can statistically separate the signal from the normal ν_μ and ν_e CC and NC background. In order to further separate the signal from the background, a set of variables which show differentiation between the two samples are used as the inputs to a feed-forward neural network (NN). The NN is configured using the TMVA package [36] with seven inputs nodes, one hidden layer with 10 nodes and one output node. Exclusive training and testing samples are selected from the MC sets to avoid bias and test for overtraining.

The variables used are (a) the log base ten of the total visible energy of the event, (b) the particle ID of the maximum energy ring in the event, (c) the number of decay electron candidates in the event, (d) the maximum distance between the primary interaction and any decay-electron found from a pion or muon decay, (e) the clustered sphericity of the event in the center of mass system, (f) the number of possible Cherenkov ring fragments, and finally (g) the fraction of total number of photo-electrons in the events carried by the first ring. The agreement between downward going data and MC (where no tau signal is expected) for the NN output along with the overlaid expected tau signal is shown in Fig. 1. See Supplemental Material at [URL will be inserted by publisher] for the additional agreement between the data and MC of the seven input variables to the NN.

All of the oscillation-induced tau neutrinos will come from below due to differing path lengths in the earth. In order avoid encoding such up-down biases into the network, and to select events based solely on their topology, the training is performed by weighting the oscillation probabilities of all events based on their energies alone, not their direction. In this way, all oscillation probabilities are correct on average, but upward-going and downward-going events are treated the same in the training process. This technique has the added benefit of not setting the weights of the down-going signal events to zero, thus preserving MC statistics. The training is performed such that an NN output which is near 1.0 signifies that the event is tau-like, while events near 0.0 are non-tau like. After training, the NN is found to efficiently separate the tau appearance signal from the background of other atmospheric neutrino interactions.

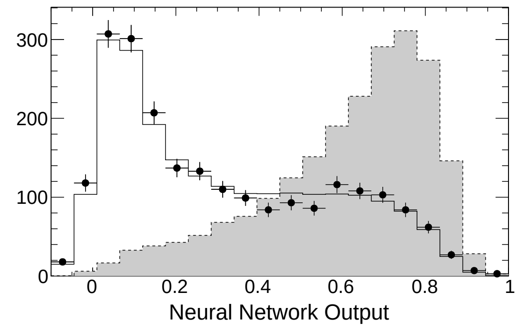

FIG. 1. The separation of signal and background by the neural network. The downward going data (points) are overlaid with the downward going atmospheric MC (solid line). Also shown is the tau signal MC (shaded). The tau signal is normalized for equal statistics.

When acting on the events passing the pre-selection cuts, 75% of the signal events (60% total efficiency) and only 26% of the background events (6% total efficiency) remain when events with a NN output of greater than 0.5 are considered. In this "tau-like" sample, NC background makes up 26% of the sample and is an important remaining background. Table I further displays the fractional breakdown of the interaction modes in the sample. In order to extract maximum information from the event samples, instead of cutting on the NN output, the output of the NN is combined with the zenith direction of the event into a probability distribution functions (PDF) and is used to jointly fit the tau and background components.

Interaction Mode	NN < 0.5	NN > 0.5	All
CC ν_e	781.4 (0.40)	381.3 (0.46)	1162.7 (0.42)
CC ν_μ	1070.2 (0.55)	200.2 (0.24)	1270.4 (0.46)
CC ν_τ	12.4 (0.01)	37.2 (0.04)	49.7 (0.02)
NC	95.2 (0.05)	209.3 (0.25)	304.4 (0.11)

TABLE I. The fractional breakdown of interaction modes of both the expected signal (CC ν_τ) and background for the SK-I period. For fitting purposes the entire sample is used in the analysis, but the NN enhanced (NN >0.5) and depleted (NN<0.5) signal selections are shown here to demonstrate the effect of signal and background separation. For each sample, the number of selected SK-I MC events is shown scaled by the 1489 days of SK-I live-time. The fractional breakdown by interaction mode of each sample is shown in parentheses.

An example of the two-dimensional distributions of the NN output versus the direction of the detected events used to discriminate signal from background is shown in Fig. 2. Distributions for both oscillation-generated taus on the left, and other atmospheric background on the right are shown. The vertical axes of these two-dimensional distributions contain the output of the NN and reflects how tau-like the event is (NN output near 1.0 tau-like, 0.0 non tau-like). The horizontal-axis is the cosine of the reconstructed zenith angle of the event which is

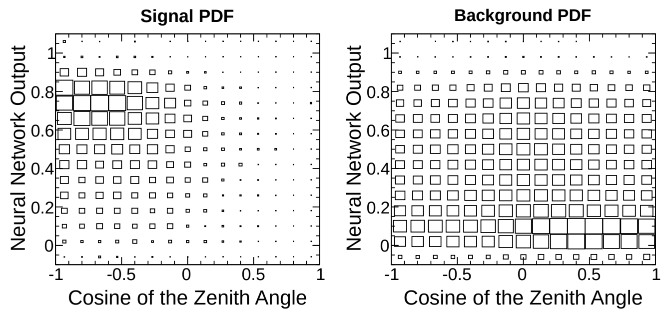

FIG. 2. Histograms of the PDFs of both tau signal (left) and atmospheric background (right). The vertical axis is the output of the NN, the horizontal axis the cosine of the event zenith direction. Upward going events are to the left, downward going to the right. The tau signal appears in the upward-going tau-like region.

determined by an energy-weighted sum of the ring directions in the event. The tau events (left panel) are indicated as tau-like by the NN and come from below ($\cos(\theta)$ near -1.0) as expected. In contrast, other atmospheric neutrinos (right panel) are primarily non-tau-like and come from both above and below. In fact, it can be seen that these events are depleted in the upward-going direction due to their oscillation into (mostly non-interacting) tau-neutrinos. By varying the relative normalization of the two distributions both the amount of tau appearance and the overall background level can be adjusted.

PDFs for each run period for both signal and background are built out of two-dimensional histograms prepared from the MC, with the probability density following the normalized bin contents. Then, an un-binned likelihood fit of the data is done to the sum of the signal and background PDFs varying the normalization between them. It is necessary to perform an un-binned fit as statistics of bins in the full two dimensional space would be quite low. The result of the fit is a normalization factor on the signal and the background which tell us how many tau interaction are needed to be consistent with our data set. Separate PDFs are produced for SK-I, II and III, and each data set is fit to its appropriate MC set. The data sets are fit both individually for each run period, and jointly together.

Although the technique employed here is more sophisticated than that of [18], it is also more sensitive to some systematic errors since large numbers of background events remain in the non-signal regions of the fitting space which were previously removed by cuts. By training the NN to recognize tau interactions, the NN also learns to effectively separate quasi-elastic (QE) from multi-pi and DIS interactions in the background samples. This is because the DIS events tend to have many extra pions in them, and thus look more like the tau signal. The DIS portion of the interactions thus form a large part of the background in the signal region and we therefore explicitly take into account uncertainties in the DIS normalization in the fit.

The average neutrino energy in the DIS interactions in our sample is 14 GeV and the cross section is not known to better than the 10% level at that energy. We also know that the application of the Bodek-Yang corrections [35] tends to suppress our DIS interactions at higher energies by about 5%. For this reason, the DIS error is introduced into the fit as a 10% gaussian error constraint. After the fit is completed it is found that the amount of DIS is increased from its nominal value by 10% at the best fit point. If the fit is performed with no constraint on the DIS fraction at all, then the DIS fraction fits 14% higher than the nominal value.

The fit is performed on each data period separately, and is also performed jointly with all data periods being fit at the same time. In the case of finding the exact normalization as predicted by the MC these factors would be 1.0. When the data periods are fit together, the tau normalization is found to be 1.42 ± 0.35 $(stat)$ with the background normalization 0.94 ± 0.02 $(stat)$. When fit separately, the tau normalizations are found to be 1.27 ± 0.49 $(stat)$, 1.47 ± 0.62 $(stat)$ and 2.16 ± 0.78 $(stat)$ for SK-I, SK-II and SK-III respectively.

It is also instructive to examine the results of the combined fit graphically. Binned projections of the fitted results can illustrate the quality and features of the fit. Figure 3 shows the projections in zenith for both tau-like (NN output > 0.5) and non-tau-like (NN output < 0.5) events, along with the projections in NN output for both upward going ($\cos(\theta) > 0.1$) and downward-going ($\cos(\theta) < 0.1$) events. In these plots the PDFs have been rescaled to the fitted normalization values. The fitted tau signal is shown in grey. Good agreement is seen in all distributions. As expected, tau events are observed as an excess of tau-like events in the upward-going direction. In these plots the PDFs and data sets from all of the run periods have been combined together.

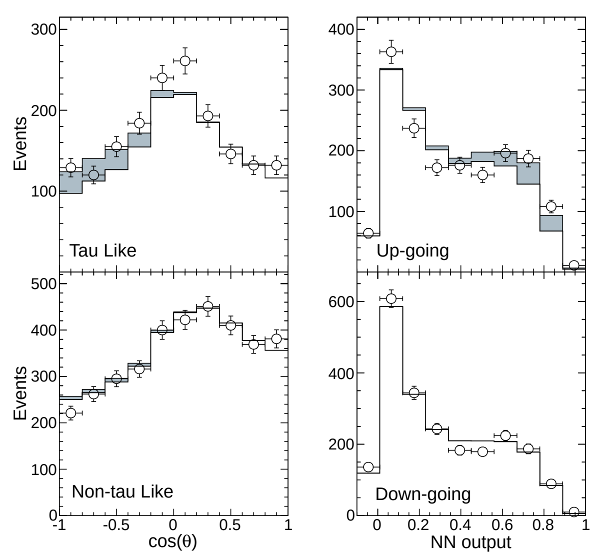

FIG. 3. Fit results showing projections in the NN output and zenith angle distribution for tau-like (NN>0.5), upward going ($\cos(\theta) > 0.1$), non-tau-like (NN<0.5), and downward going ($\cos(\theta) < 0.1$) events for both the two-dimensional PDFs and data. The PDFs and data-sets have been combined from SK-I through SK-III in this figure. The fitted tau signal is shown in grey.

There are 28 uncertainties which are a subset of those used in the Super-K three-flavor atmospheric neutrino analysis. A more detailed description of them can be found in [24]. The systematic errors for the analysis are divided into two sets. The first set, which describes errors on the tau expectation itself, plays no role in comparing the fitted observed number of events with the no-tau appearance hypothesis and does not affect the significance of this quoted result. However, this set is used to quote an error on the expected number of events and includes uncertainties in ν_τ cross section, and any uncertainty that would increase both the signal and the background in a way that does not change the significance of the reported result. Detector biases on selection and fitting are included in these uncertainties but are quite small compared to the tau cross-section error, the largest being a 5% error on the detector energy scale. The error on the tau cross-section was made by a comparison of NEUT [28] with several other models, looking in particular at the differences between NEUT and the cross-section model by Hagiwara *et al* [33]. Another comparison between cross-section models was recently completed by the authors of [20] and gave similar results. As noted above, this 25% error does not contribute to the reported significance of this letter. However, future analysis using this high statistics data set employing full simultaneous treatment of all relevant systematic errors can measure this cross-section and constrain its uncertainty using the Super-K data itself.

The second class of errors includes those that would affect the observed signal but not the background, or otherwise would cause the significance of the measured normalization to change when doing the fit. There are five such errors: the up/down flux ratio, the horizontal/vertical flux ratio, the K/π flux ratio, the NC/CC cross-section ratio, and the up/down energy scale difference in the detector. In the current analysis the dominant error on the signal was the NC/CC ratio changing the fitted number of events of about $\pm 7\%$ due to the relatively large percentage of NC background in the signal region.

Also included in the errors which can change the measured results and significance are those due to variations in the known oscillation parameters. For this study they are varied within the 1σ limits of a combined SK-I+SK-II+SK-III atmospheric oscillation analysis results assuming the normal hierarchy [25]. The Δm^2_{32} is varied between 1.92×10^{-3} and $2.22 \times 10^{-3}\mathrm{eV}^2$, $\sin^2 2\theta_{23}$ is varied between 0.93 and 1.0. The θ_{13} values are varied within our combined Daya Bay [15] and RENO [16] results of $\sin^2 2\theta_{13} = 0.099 \pm .014$. The use of non-zero θ_{13} results in a 13% reduction of the fitted normalization as three flavor oscillations produce high energy upward going electron neutrinos which add to the upward-going background, thus decreasing the needed number of tau neutrinos to explain the signal region. However, the variation in θ_{13} around this central value results in less than a 1% change in the fit result. For this analysis, we set the value of δ_{CP} to zero. Varying the value of δ_{CP} results in, at most, a 1.3% difference in the number of fitted taus, and we neglect this uncertainty. The systematic errors are summarized in Table II.

Systematics Uncertainties for ν_τ normalization		$+$ %	$-$ %
Super-K atmospheric ν oscillation errors			
28 error terms	(expected events)	13.4	14.7
5 error terms	(observed events)	7.9	8.5
Tau neutrino cross section	(expected events)	25.0	25.0
Oscillation parameters	(observed events)	5.4	1.3

TABLE II. Summary of systematic uncertainties for both the expected and observed number of ν_τ events. The errors for each category including that of the oscillation parameters have been added in quadrature.

Including and combining the observed (+9.6 -8.6%) and expected (+28.4 -30.0%) systematic uncertainties separately, the fitted value of the tau normalization is $1.42 \pm 0.35\ (stat)\ ^{+0.14}_{-0.12}\ (sys)$. After rescaling the MC by all fitting factors and correcting for efficiency, the observed number of fitted events over the entire running period is calculated to be $180.1 \pm 44.3\ (stat)\ ^{+17.8}_{-15.2}\ (sys)$ events. This is to be compared to an expectation of $120.2\ ^{+34.2}_{-34.8}\ (sys)$ interactions in the fiducial volume if no fitting factors are applied. Identifying this large statistics sample opens the possibility to study charged current tau neutrino interaction physics with oscillation produced tau neutrinos.

The observed number of events is converted to the significance level at which we can reject the no-tau-appearance hypothesis. The measured signal normalization (1.42 and its associated statistical and systematic errors) is compared with the case of no ν_τ appearance, which would have a normalization of zero. An asymmetric gaussian centered at 1.42 is prepared and the integral of the PDF below zero is calculated. The p-value is 6.2×10^{-5} which corresponds to a significance level of 3.8σ. A significance of 2.7σ is expected for the nominal expected signal. The larger measured significance is a consequence of the fact that more signal was measured than expected. The DIS fraction is fit with a 10% increase over its nominal value, and is correlated with the tau normalization. Because of this, not only is the fitted tau normalization lower than it would be without this error, but the error on the tau normalization is larger than it would otherwise be due to the presence of the correlated DIS error, thus slightly reducing the measured significance. It should be noted that if the inverted hierarchy is chosen instead of the normal one when calculating the oscillation probabilities, the expected number of θ_{13}-induced upward going electrons is reduced, approximately in half, resulting in a somewhat higher fitted value (1.56) and a correspondingly higher significance.

In summary, we find that the Super-Kamiokande atmospheric neutrino data is best described by neutrino oscillations that includes tau neutrino appearance in addition to the overwhelming signature of muon neutrino disappearance. By a neural network analysis on the zenith angle distribution of multi-GeV contained events, we have demonstrated this at a significance of 3.8σ.

We gratefully acknowledge the cooperation of the Kamioka

Mining and Smelting Company. The Super-Kamiokande experiment has been built and operated from funding by the Japanese Ministry of Education, Culture, Sports, Science and Technology, the United States Department of Energy, and the U.S. National Science Foundation.

---

* Deceased.
† Present address: GIST College, Gwangju Institute of Science and Technology, Gwangju 500-712, Korea
‡ Present address: Department of Physics and Astronomy, University of Minnesota, MN, 55455, USA

[1] Y. Fukuda *et al.* (Super-Kamiokande Collaboration), Phys.Rev.Lett. **81**, 1562 (1998), arXiv:hep-ex/9807003 [hep-ex].
[2] Y. Ashie *et al.* (Super-Kamiokande Collaboration), Phys.Rev. **D71**, 112005 (2005), arXiv:hep-ex/0501064 [hep-ex].
[3] J. Hosaka *et al.* (Super-Kamkiokande Collaboration), Phys.Rev. **D73**, 112001 (2006), arXiv:hep-ex/0508053 [hep-ex].
[4] K. Abe *et al.* (Super-Kamiokande Collaboration), Phys.Rev. **D83**, 052010 (2011), arXiv:1010.0118 [hep-ex].
[5] Q. Ahmad *et al.* (SNO Collaboration), Phys.Rev.Lett. **89**, 011301 (2002), arXiv:nucl-ex/0204008 [nucl-ex].
[6] B. Aharmim *et al.* (SNO Collaboration), Phys.Rev. **C81**, 055504 (2010), arXiv:0910.2984 [nucl-ex].
[7] B. Aharmim *et al.* (SNO Collaboration), (2011), arXiv:1109.0763 [nucl-ex].
[8] S. Abe *et al.* (KamLAND Collaboration), Phys.Rev.Lett. **100**, 221803 (2008), arXiv:0801.4589 [hep-ex].
[9] M. Ahn *et al.* (K2K Collaboration), Phys.Rev. **D74**, 072003 (2006), arXiv:hep-ex/0606032 [hep-ex].
[10] P. Adamson *et al.* (MINOS Collaboration), Phys.Rev.Lett. **101**, 131802 (2008), arXiv:0806.2237 [hep-ex].
[11] K. Abe *et al.* (T2K Collaboration), Phys.Rev. **D85**, 031103 (2012), arXiv:1201.1386 [hep-ex].
[12] K. Abe *et al.* (T2K Collaboration), Phys.Rev.Lett. **107**, 041801 (2011), arXiv:1106.2822 [hep-ex].
[13] P. Adamson *et al.* (MINOS Collaboration), Phys.Rev.Lett. **107**, 181802 (2011), arXiv:1108.0015 [hep-ex].
[14] Y. Abe *et al.* (DOUBLE-CHOOZ Collaboration), Phys.Rev.Lett. **108**, 131801 (2012), arXiv:1112.6353 [hep-ex].
[15] F. An *et al.* (DAYA-BAY Collaboration), Phys.Rev.Lett. **108**, 171803 (2012), arXiv:1203.1669 [hep-ex].
[16] J. Ahn *et al.* (RENO Collaboration), Phys.Rev.Lett. **108**, 191802 (2012), arXiv:1204.0626 [hep-ex].
[17] The OPERA Collaboration, (2011), arXiv:1107.2594 [hep-ex].
[18] K. Abe *et al.* (Super-Kamiokande Collaboration), Phys.Rev.Lett. **97**, 171801 (2006), arXiv:hep-ex/0607059 [hep-ex].
[19] P. Migliozzi and F. Terranova, New J.Phys. **13**, 083016 (2011), arXiv:1107.3018 [hep-ex].
[20] J. Conrad, A. de Gouvea, S. Shalgar, and J. Spitz, Phys.Rev. **D82**, 093012 (2010), arXiv:1008.2984 [hep-ph].
[21] Y. Fukuda *et al.*, Nucl. Instrum. Meth. **A501**, 418 (2003).
[22] M. Honda, T. Kajita, K. Kasahara, and S. Midorikawa, Phys.Rev. **D70**, 043008 (2004), arXiv:astro-ph/0404457 [astro-ph].
[23] `http://www.phy.duke.edu/~raw22/public/Prob3++`.
[24] R. Wendell *et al.* (Super-Kamiokande Collaboration), Phys.Rev. **D81**, 092004 (2010), arXiv:1002.3471 [hep-ex].
[25] K. Abe *et al.* (Super-Kamiokande Collaboration), Phys.Rev.Lett. **107**, 241801 (2011), arXiv:1109.1621 [hep-ex].
[26] T. Schwetz, M. Tortola, and J. Valle, New J.Phys. **13**, 109401 (2011), arXiv:1108.1376 [hep-ph].
[27] P. Adamson *et al.* (MINOS Collaboration), Phys.Rev.Lett. **106**, 181801 (2011), arXiv:1103.0340 [hep-ex].
[28] Y. Hayato, Nucl. Phys. Proc. Suppl. **112**, 171 (2002).
[29] R. Brun, F. Bruyant, M. Maire, A. McPherson, and P. Zanarini, "GEANT3," (1987).
[30] C. Berger and L. Sehgal, Phys.Rev. **D76**, 113004 (2007), arXiv:0709.4378 [hep-ph].
[31] D. Rein and L. Sehgal, Phys.Lett. **B657**, 207 (2007), arXiv:hep-ph/0606185 [hep-ph].
[32] S. Jadach, Z. Was, R. Decker, and J. H. Kuhn, Comput. Phys. Commun. **76**, 361 (1993).
[33] K. Hagiwara, K. Mawatari, and H. Yokoya, Nucl. Phys. **B668**, 364 (2003), hep-ph/0305324.
[34] M. Gluck, E. Reya, and A. Vogt, Z.Phys. **C67**, 433 (1995).
[35] A. Bodek and U. Yang, Nucl.Phys.Proc.Suppl. **112**, 70 (2002), arXiv:hep-ex/0203009 [hep-ex].
[36] A. Hocker, J. Stelzer, F. Tegenfeldt, H. Voss, K. Voss, *et al.*, PoS **ACAT**, 040 (2007), arXiv:physics/0703039 [PHYSICS].